

Understanding Programming of Fungal Iterative Polyketide Synthases: the Biochemical Basis for Regioselectivity by the Methyltransferase Domain in the Lovastatin Megasyntase

Ralph A. Cacho, Justin Thuss, Wei Xu, Randy Sanichar,
Zhizeng Gao, Allison Nguyen, John C. Vederas, and Yi Tang

J. Am. Chem. Soc., **Just Accepted Manuscript** • DOI: 10.1021/jacs.5b11814 • Publication Date (Web): 02 Dec 2015

Downloaded from <http://pubs.acs.org> on December 9, 2015

Just Accepted

“Just Accepted” manuscripts have been peer-reviewed and accepted for publication. They are posted online prior to technical editing, formatting for publication and author proofing. The American Chemical Society provides “Just Accepted” as a free service to the research community to expedite the dissemination of scientific material as soon as possible after acceptance. “Just Accepted” manuscripts appear in full in PDF format accompanied by an HTML abstract. “Just Accepted” manuscripts have been fully peer reviewed, but should not be considered the official version of record. They are accessible to all readers and citable by the Digital Object Identifier (DOI®). “Just Accepted” is an optional service offered to authors. Therefore, the “Just Accepted” Web site may not include all articles that will be published in the journal. After a manuscript is technically edited and formatted, it will be removed from the “Just Accepted” Web site and published as an ASAP article. Note that technical editing may introduce minor changes to the manuscript text and/or graphics which could affect content, and all legal disclaimers and ethical guidelines that apply to the journal pertain. ACS cannot be held responsible for errors or consequences arising from the use of information contained in these “Just Accepted” manuscripts.

Understanding Programming of Fungal Iterative Polyketide Synthases: the Biochemical Basis for Regioselectivity by the Methyltransferase Domain in the Lovastatin Megasyntase

Ralph A. Cacho,^{1‡} Justin Thuss,^{2‡} Wei Xu,¹ Randy Sanichar,² Zhizeng Gao,² Allison Nguyen,¹ John C. Vederas,² Yi Tang¹

¹Department of Chemical and Biomolecular Engineering, Department of Chemistry and Biochemistry, University of California, Los Angeles, CA 90095, USA; ²Department of Chemistry, University of Alberta, Edmonton, AB, Canada T6G 2G2

Supporting Information Placeholder

ABSTRACT: Highly-reducing polyketide synthases (HR-PKSs) from fungi synthesize complex natural products using a single set of domains in a highly programmed, iterative fashion. The most enigmatic feature of HR-PKSs is how tailoring domains function selectively during different iterations of chain elongation to afford structural diversity. Using the lovastatin nonaketide synthase LovB as a model system and a variety of acyl substrates, we characterized the substrate specificity of the LovB methyltransferase (MT) domain. We showed that while the MT domain displays methylation activity toward different β -ketoacyl groups, it is exceptionally selective towards its naturally programmed β -keto-dienyltetraketide substrate with respect to both chain length and functionalization. Accompanying characterization of the ketoreductase (KR) domain displays broader substrate specificity towards different β -ketoacyl groups. Our studies indicate that selective modifications by tailoring domains, such as the MTs, are achieved by higher kinetic efficiency on a particular substrate relative to the rate of transformation by other competing domains.

Fungal highly-reducing polyketide synthases (HR-PKSs) are multidomain megasyntases that are involved in the biosynthesis of diverse polyketide natural products, highlighted by the cholesterol lowering agent lovastatin and the protein transport inhibitor brefeldin A.^{1,2} HR-PKSs contain a linearly juxtaposed set of domains that iteratively build the polyketide chain through decarboxylative condensation and β -ketoacyl functionalization. In each HR-PKS, a single set of domains is repeatedly and permutatively used through chain elongation cycles to yield the final product. These programmed tailoring steps are precisely executed by the HR-PKSs to afford richly functionalized polyketide chains that set up post-PKS modifications and afford diverse biological activities. For example, during the synthesis of dihydromonacolin L (DML), the precursor to lovastatin, the lovastatin nonaketide synthase LovB performs eight cycles of chain extension and tailoring (Figure 1).^{3,4} The orchestration of different tailoring activities sets up key structural features in DML, including the decalin core that is proposed to derive from a triene hexaketide intermediate through Diels-Alder cyclization;⁵ and the terminal β -hydroxy acid moiety that is important for inhibition of HMG-CoA reductase.⁶ Compared to bacterial counterparts that function in a well-understood assembly-line like fashion,⁷ these complex biochemical features of fungal HR-

PKSs remain unresolved. Knowledge of how tailoring domains function will enable both rational manipulation of the megasyntases,^{8,9} and product prediction from the vast number of HR-PKSs uncovered through genome sequencing efforts.

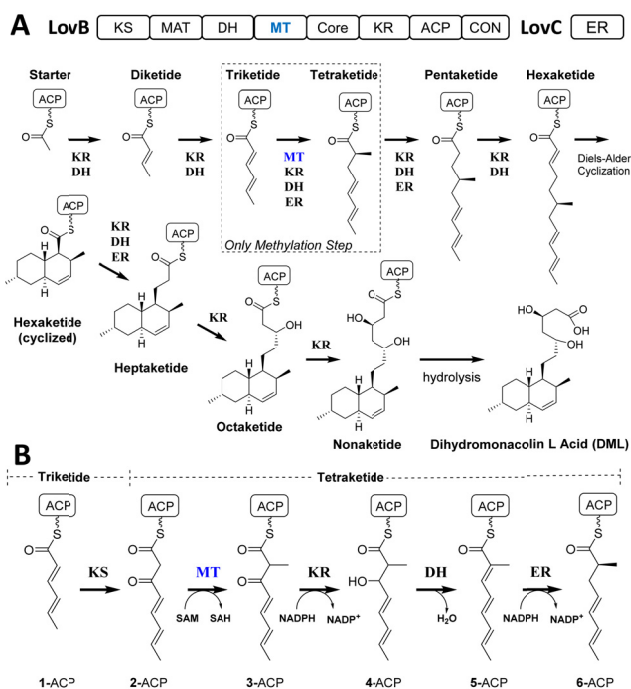


Figure 1. The programmed steps of LovB in the synthesis of dihydromonacolin L (DML). (A) The catalytic steps by LovB; LovB is a HR-PKS and LovC is the dissociated enoylreductase; and (B) the tetraketide modification steps shown in detail highlighting the timing of the MT domain. Domain abbreviations: ketosynthase (KS); malonyl-CoA:ACP acyltransferase (MAT); α -methyltransferase (MT), β -ketoreductase (KR), dehydratase (DH), α - β enoylreductase (ER), acyl carrier protein (ACP) and NRPS-like Condensation (CON).

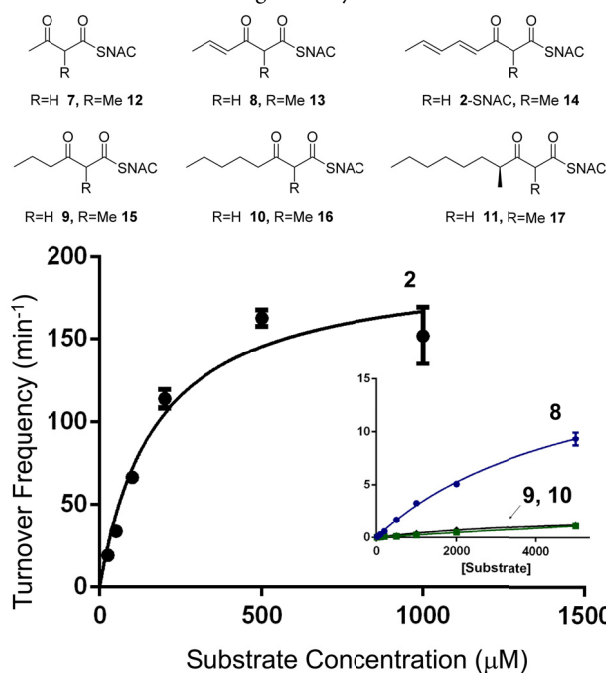
The α -methylation of β -ketoacyl-*S*-ACP intermediate is a commonly observed modification during selected cycles of HR-PKSs.^{1,10-12} The reaction is catalyzed by an in-line methyltransferase (MT) domain using *S*-adenosylmethionine (SAM) as a cofactor immediately following ketosynthase (KS)-catalyzed chain elonga-

tion, and occurs prior to β -reductive modifications performed by ketoreductase (KR), dehydratase (DH) and enoylreductase (ER) domains. During the eight chain elongation and tailoring iterations catalyzed by LovB, the MT domain is apparently only active during the conversion of tetraketide 2-ACP to the on-pathway intermediate 6-ACP, with the α -methyl 3-ACP being the product of the MT. Curiously, no methylation modification occurs on other β -ketoacyl-S-ACP substrates in the other catalytic cycles of LovB (Figure 1). However, α -methylation of the tetraketide is essential for the remaining steps of the pathway shown in Figure 1A, as the dissociated ER LovC is unable to recognize the α -desmethyl version of 5-ACP and the entire catalytic cascade subsequently derails.^{3,13} The importance of methylation modification on the fidelity of other iterative HR-PKs has also been observed, in which bypassing programmed MT function results in production of shunt products.¹⁴ Therefore, the HR-PKs have clearly evolved to optimize the timing and regioselectivities of the MT domains.

We hypothesize that two possible mechanisms of substrate processing can account for LovB MT selectivity. First, the HR-PKs may adopt an assembly-line like model in which each substrate is passed through the way stations sequentially in the order of MT->KR->DH->ER. In the case of LovB, the MT domain only recognizes 2-ACP while excluding all of the other substrates completely. Alternatively in a kinetically controlled mechanism, we propose that once formed and released from the KS, the β -ketoacyl-S-ACP substrate can sample all potential modifying domains, including the MT, KR and KS. The outcome of the tailoring steps is determined by the relative activities of each domain towards the substrate. The MT domain is primarily in competition with the KR domain for the substrate: if a substrate is readily reduced by the KR domain first, then no methyl transfer will be possible. Conversely, a higher MT activity relative to the KR will lead to methylation prior to reduction. To understand the basis for the MT selectivity, individual rates of the MT and KR domain towards the different β -ketoacyl-S-ACP substrates need to be measured and compared.

We synthesized a panel of acyl-S-N-acetylcysteamine (SNAC) compounds as substrates for the MT and KR assays. The majority of the β -ketoacyl-SNAC compounds (Figure 2) were prepared using titanium-catalyzed aldol chemistry to synthesize β -hydroxycarbonyl species that were further functionalized and oxidized to provide the desired β -carbonyl SNAC esters (Supporting Information).^{15,16} Access to shorter, saturated SNAC esters was achieved using acylated Meldrum's acid.^{17,18} The acyl portions of the substrates vary in chain length from diketide (C4) to pentaketide (C10) as well as functionalization. Compounds 7, 8 and 2 represent the natural β -ketoacyl intermediates in the LovB catalytic cycle, while compounds 9-11 are model, simplified substrates. We also synthesized the corresponding α -methyl- β -ketoacyl products 12-17 as standards for quantifying the methylation product amount (Supporting Information). The synthetic strategy outlined above was expanded to include the α -methylated SNAC esters. Rapid ketonol interconversion excluded the need for stereoselective methylation (Supporting information). Furthermore, a number of β -hydroxylacyl-SNAC compounds were synthesized and used as standards for the ketoreduction assay (Supporting Information). These standards were conveniently obtained as intermediates in the synthesis of compounds 2, 7-17. Intact LovB was expressed and purified from *Saccharomyces cerevisiae* strain BJ5464-NpgA as previously described and used in the assays at final concentrations

between 0.01 and 1 μ M.⁴ To allow for quantification and prevent further tailoring reactions of the KR products in the assay, we constructed a point mutation H985A in the DH domain of LovB to yield LovB-DH^o (Figure S1).¹⁹ LC-MS based product quantification was employed for both the methylation (containing SAM) and ketoreduction (containing NADPH) assays, using standard curves constructed from the mass signals of synthesized standards.



entry	k_{cat} (min ⁻¹)	K_M (mM)	k_{cat}/K_M (min ⁻¹ mM ⁻¹)	Relative activity (%)
8	2.50 \pm 0.17	5.60 \pm 0.56	0.48 \pm 0.06	0.04
9	11.5 \pm 4.4	47.0 \pm 19.8	0.24 \pm 0.14	0.02
10	19.0 \pm 1.2	5.20 \pm 0.53	3.60 \pm 0.37	0.3
2	195.5 \pm 11.4	0.17 \pm 0.03	1136 \pm 202	100

Figure 2. Full kinetic analysis of LovB MT domain towards different β -ketoacyl-SNAC substrates. **2** is the natural tetraketide substrate based on DML structure. **8** is the on-pathway triketide substrate of LovB. No reaction towards diketide **7** or pentaketide **11** was observed.

We first assayed the activity of the MT domain towards the natural tetraketide **2**. Overnight incubation of 2 mM of **2** in the presence of SAM led to complete consumption of the substrate and the appearance of **14**. Michaelis-Menten saturation kinetics assay gave a robust k_{cat} of 196 min⁻¹ and K_M of 170 μ M (Figures 2 and S8). The K_M value was surprisingly low considering acyl-SNAC mimic of the ACP-bound substrates can suffer from significant penalties in K_M due to loss of protein-protein interactions, and are typically in the millimolar range.^{11,20,21} Hence the kinetic parameters of **2** suggest that the natural tetraketide can bind exceptionally well to the active site MT domain of LovB. Having demonstrated the MT domain activity can be confirmed with **2**, we then tested MT catalysis towards β -ketoacyl-SNAC substrates of varying chain lengths. No significant (<1%) methylation can be observed with either the natural diketide **7** or the model pentaketide substrate **11**. The failure to methylate **7** is in contrast to that of the chaetoviridin HR-PKs MT domain, which naturally methylates β -ketobutyryl-ACP intermediate as well as **7** in the same assay.²² The MT domain showed noticeable activity towards converting triketide **8** to **13**, albeit significantly attenuated compared to that towards **2**. Kinetic

analysis showed the MT displays a 2500-fold drop in catalytic efficiency towards **8** compared to **2**, which resulted from ~50-fold attenuation in both the k_{cat} and K_M values (Figure S10).

We next assayed the substrate preference of LovB MT towards more simplified substrates such as the saturated **10** and **9**. While conversion of **10** to **16** was confirmed by using a standard of **16**, a surprising penalty to the catalytic efficiency (0.3% of **2**) was observed including a 10-fold decrease in k_{cat} and nearly 40-fold increase in K_M (Figure S9). A 7.5-fold drop in catalytic efficiency compared to **8** was also observed when the γ - δ double bond was saturated in the triketide **9** (Figure S11). Collectively, our methylation assays with LovB MT domain point to exceptional substrate specificity towards the natural 3-oxo-oct-4,6-dienyl acyl group. Changes to chain length and functionalization both resulted in significant decreases in the methylation rate. The requirement of correct substrate functionalization further suggests that the MT domain itself can act as a gatekeeping domain in the programming of LovB. In the event that other tailoring domains malfunction in the previous cycles and present an alternative substrate, the MT domain activities will be significantly attenuated. This would likely result in enzyme stalling or ketoreduction (bypassing the MT function) of the substrate, which will eventually result in off-loading of the polyketide product as previously demonstrated.⁴

Having established the substrate scope and kinetic properties of the MT domain, we next assayed the properties of the KR domain towards the tri- and tetraketide substrates. Since the KR is functional in every iteration of the HR-PKS, we expect the substrate specificities towards different β -ketoacyl thioesters to be more relaxed. We used the MS-based quantification of substrate conversion, similar to that used in the MT assay. However, significant difficulties were encountered when working with the conjugated β -ketoacyl substrates such as **2** and **8**, due to i) broadening of the peak as a result of enolization of the β -keto group; ii) retention time overlap; iii) MS signal overlap due to isotopic abundance of the substrate and the actual mass of the product; and iv) spontaneous dehydration of the β -hydroxyl product (see Figure 3B). Therefore, we used model substrates **9**, **15**, **10** and **16** to perform the kinetics assays. The α -methyl compounds **15** and **16** were chosen to examine the effect of methylation of substrate specificity. Following overnight incubation in the presence of NADPH and confirmation of product formation using synthesized standards, we performed time-course analysis using single substrate concentration of 1 mM and enzyme concentration of 5 μM to obtain the apparent turnover rates as shown in Table 1. We also attempted to obtain saturation kinetics of the KR domain towards the substrates, however we were not able to reach saturation at solubility limits of the substrate with the exception of **9** which gave k_{cat} of 34.3 min^{-1} and K_M of 2 mM ($k_{\text{cat}}/K_M = 18.5 \text{ min}^{-1}\text{mM}^{-1}$) (Figure S12). Fitting the linear region of the kinetics data of **10** yielded a k_{cat}/K_M value of 5.4 $\text{min}^{-1}\text{mM}^{-1}$ (Figure S13). Although we were not able to obtain full kinetic data on all of the substrates of interest, one can still conclude based on Table 1 that the KR domain does not differentiate between different substrates significantly (within an order of magnitude). The activity of KR is also not significantly affected by the presence of the α -methyl group, suggesting that KR does not exert any significant kinetic penalty towards a noncognate substrate. This further suggests the importance of substrate specificity at the MT step to determine the first tailoring reaction of the β -ketoacyl substrate.

Table 1. Apparent Turnover rate of LovB KR domain.^a

Substrate	9	15	10	16
Turnover (min^{-1})	16.1 \pm 0.5	5.1 \pm 0.4	2.1 \pm 0.02	2.4 \pm 0.1

^a Substrate concentration at 1 mM, enzyme concentration at 5 μM .

While the acyl-SNAC substrates enabled a relative measure of the domain specificity towards different acyl groups, these remain a much-simplified model of the actual ACP-bound intermediates that are *in cis* with all the tailoring domains. To determine if there is indeed competitive catalysis between the KR and MT domains towards the β -ketoacyl substrates, we performed a combined MT/KR assay in which each substrate (**2**, **8-10**) was added to LovB DH^o mutant in the presence of both SAM and NADPH, and the amounts of each product was compared. The MT-first products can be both the α -methyl- β -keto (+14 mu) and the α -methyl- β -hydroxyl (+16 mu) compounds, the latter represent the products of ketoreduction following methylation. The KR-first products are the β -hydroxyl compounds (+2 mu) of which the MT domain can no longer methylate.

We first analyzed the competitive modification of model substrates **9** and **10** since all the products can be quantified using standards. As shown in Figure 3A and Figures S14-15, when **9** was used in the assay in the presence of equimolar amounts of SAM and NADPH, the amount of KR products are significantly more than the MT products (MT/KR product ratio of 1:4) when quantified after three hours. This is consistent with the individually determined kinetic parameters of which the KR is more active towards triketide **9**. Increasing the amount of SAM led to higher amount of the MT products. Conversely, using **10** led to the reversal of product distribution with MT/KR product ratio of 4:1. This is in spite of the kinetic assays showing comparable k_{cat}/K_M for both domains towards **10**. However, the K_M of the KR domain towards **10** is very high as we were not able to reach saturation in the assay. Hence under assay conditions of 1 mM **10**, the binding of the SNAC substrate by the KR is likely substantially weaker compared to the MT.

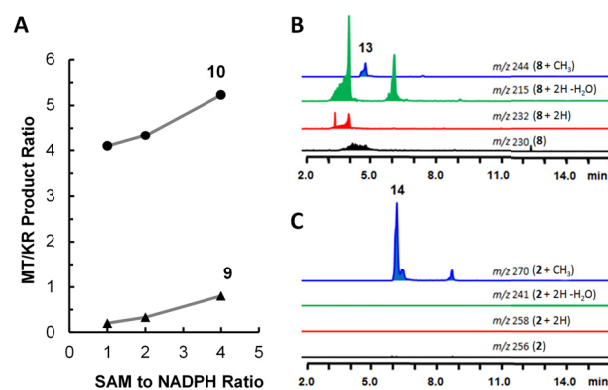


Figure 3. KR and MT competition assays using model and natural tri- and tetraketide substrates. (A) Quantification of product distribution of model substrates **9** and **10**. (B) and (C) Product distributions of natural substrates **8** and **2**, respectively. Shown are the extract ion chromatograms of different products as indicated.

The competition assays were then performed using the natural substrates **2** and **8** and analyzed by selected ion monitoring as shown in Figures 3B and 3C. When LovB DH^o was added to **8** in the presence of both SAM and NADPH, we observed a 10:1 ratio

of KR to MT-catalyzed products consistent with the natural programming rules of LovB. Most of the KR products were found to contain the m/z 215 ion and split into two major peaks. The earlier peak at $T_R \sim 4$ min is the β -hydroxyl compound (parent m/z 233 also observed) and has undergone dehydration during ionization. A standard of the β -hydroxyl compound gave an identical ionization pattern. The second peak at $T_R \sim 6$ min is the actual dehydrated dienyl-SNAC, which forms readily in aqueous solution. When the natural tetraketide **2** was used in the competition assay, only the methylated product **14** was observed. Selected ion monitoring revealed that no reduced products can be found in the assay, thereby confirming the much higher catalytic efficiency of the MT domain towards **2** compared to that of KR. Interestingly, no further β -ketoreduction of **14** can be detected in the assay. Directly using **14** in a KR-only assay also did not yield any ketoreduced products. This observation is unexpected as the acyl portion of **14** is the natural substrate of KR in the predicted programmed steps of LovB (Figure 1). Although the exact reason for this result is unresolved, one possible explanation may be recognition of the acyl portion of **14** (in the β -keto form) requires interactions with the ACP as observed in other PKS systems by NMR studies.²³

Our assays using both natural and model substrates provide an explanation for the programmed methylation step observed in the iterative cycles of LovB. We suggest the MT and KR domains compete for each of the β -ketoacyl substrates released by the KS domain, and the relative rates determine the outcome of the immediate tailoring domain choice. The MT domain of LovB has been precisely tuned to be highly selective for the natural tetraketide **2** and to outcompete the KR at this particular step only. Both chain length and functional variation in the acyl substrate can lead to substantial penalties in catalytic efficiency for the MT domain. In contrast, the KR domain appears to be less substrate dependent in terms of catalytic efficiency. As a reflection of the competition between MT and KR, a 30-fold drop in the catalytic efficiency of MT towards **10** (as compared to **2**) can lead to $\sim 20\%$ of the substrate being ketoreduced without being first methylated. As the correct methyl substitution is essential for recognition in some (but not all) downstream steps,⁴ this may pose a significant barrier to some precursor-directed biosyntheses of polyketides using HRPKSs. Particular structural variations in precursors can derail the programmed steps of the domains and lead to production of shunt products instead. However, it is clear from previous work that late steps catalyzed by LovB can proceed without methylation to make a des-methyl dihydromonacolin L.⁴

Our findings with the LovB MT domain poses intriguing questions as to how substrate specificity is achieved at the molecular level, how other MT domains in HRPKSs have alternative substrate specificities and the possible influence of the HRPKS quaternary structure in the intrinsic biosynthetic programming rules of these megasynthases. For example, in the fusarielin HRPKS,²⁴ the MT domain is functional on the di-, tri- and pentaketide intermediates, while inactive on the tetraketide. This is a complete reversal of specificity compared to LovB, and structural comparisons between the two MT domains will provide insights into their differences.

ASSOCIATED CONTENT

Supporting Information

Experimental details and synthetic procedures. This material is available free of charge via the Internet at <http://pubs.acs.org>.

AUTHOR INFORMATION

Corresponding Author

yitang@ucla.edu, john.vederas@ualberta.ca

Author Contributions

[‡]These authors contributed equally.

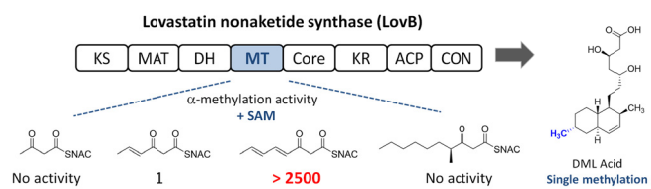
ACKNOWLEDGMENT

These investigations were supported by the by NIH (1R01GM085128 and 1DP1GM106413) YT; and the Natural Sciences & Engineering Research Council of Canada (NSERC) and by the Canada Research Chair in Bioorganic & Medicinal Chemistry to JCV.

REFERENCES

- (1) Chooi, Y. H.; Tang, Y. *J. Org. Chem.* **2012**, *77*, 9933.
- (2) Cox, R. J. *Org. Biomol. Chem.* **2007**, *5*, 2010.
- (3) Kennedy, J.; Auclair, K.; Kendrew, S. G.; Park, C.; Vederas, J. C.; Richard Hutchinson, C. *Science* **1999**, *284*, 1368.
- (4) Ma, S. M.; Li, J. W.-H.; Choi, J. W.; Zhou, H.; Lee, K. K. M.; Moorhith, V. A.; Xie, X.; Kealey, J. T.; Da Silva, N. A.; Vederas, J. C.; Tang, Y. *Science* **2009**, *326*, 589.
- (5) Auclair, K.; Sutherland, A.; Kennedy, J.; Witter, D. J.; Van den Heever, J. P.; Hutchinson, C. R.; Vederas, J. C. *J. Am. Chem. Soc.* **2000**, *122*, 11519.
- (6) Istvan, E. S.; Deisenhofer, J. *Science* **2001**, *292*, 1160.
- (7) Khosla, C.; Herschlag, D.; Cane, D. E.; Walsh, C. T. *Biochemistry* **2014**, *53*, 2875.
- (8) Kakule, T. B.; Lin, Z.; Schmidt, E. W. *J. Am. Chem. Soc.* **2014**, *136*, 17882.
- (9) Fisch, K. M.; Bakeer, W.; Yakasai, A. A.; Song, Z.; Pedrick, J.; Wasil, Z.; Bailey, A. M.; Lazarus, C. M.; Simpson, T. J.; Cox, R. J. *J. Am. Chem. Soc.* **2011**, *133*, 16635.
- (10) Winter, J. M.; Sato, M.; Sugimoto, S.; Chiou, G.; Garg, N. K.; Tang, Y.; Watanabe, K. *J. Am. Chem. Soc.* **2012**, *134*, 17900.
- (11) Xie, X.; Meehan, M. J.; Xu, W.; Dorrestein, P. C.; Tang, Y. *J. Am. Chem. Soc.* **2009**, *131*, 8388.
- (12) Eley, K. L.; Halo, L. M.; Song, Z.; Powles, H.; Cox, R. J.; Bailey, A. M.; Lazarus, C. M.; Simpson, T. J. *Chembiochem* **2007**, *8*, 289.
- (13) Ames, B. D.; Nguyen, C.; Bruegger, J.; Smith, P.; Xu, W.; Ma, S.; Wong, E.; Wong, S.; Xie, X.; Li, J. W.-H.; Vederas, J. C.; Tang, Y.; Tsai, S.-C. *Proc. Natl. Acad. Sci. U. S. A.* **2012**, *109*, 11144.
- (14) Zou, Y.; Xu, W.; Tsunematsu, Y.; Tang, M.; Watanabe, K.; Tang, Y. *Org. Lett.* **2014**, *16*, 6390.
- (15) Mikami, K.; Matsukawa, S. *J. Am. Chem. Soc.* **1993**, *115*, 7039.
- (16) Ge, H.-M.; Huang, T.; Rudolf, J. D.; Lohman, J. R.; Huang, S.-X.; Guo, X.; Shen, B. *Org. Lett.* **2014**, *16*, 3958.
- (17) Oikawa, Y.; Sugano, K.; Yonemitsu, O. *J. Org. Chem.* **1978**, *43*, 2087.
- (18) Piasecki, Shawn K.; Taylor, Clint A.; Detelich, Joshua F.; Liu, J.; Zheng, J.; Komsoukianians, A.; Siegel, Dionicio R.; Keatinge-Clay, Adrian T. *Chem. Biol.* **2011**, *18*, 1331.
- (19) Keatinge-Clay, A. *J. Mol. Biol.* **2008**, *384*, 941.
- (20) Wu, N.; Tsuji, S. Y.; Cane, D. E.; Khosla, C. *J. Am. Chem. Soc.* **2001**, *123*, 6465.
- (21) Yin, Y.; Lu, H.; Khosla, C.; Cane, D. E. *J. Am. Chem. Soc.* **2003**, *125*, 5671.
- (22) Winter, J. M.; Chiou, G.; Bothwell, I. R.; Xu, W.; Garg, N. K.; Luo, M.; Tang, Y. *Org. Lett.* **2013**, *15*, 3774.
- (23) Evans, S. E.; Williams, C.; Arthur, C. J.; Płoskoń, E.; Wattanamorn, P.; Cox, R. J.; Crosby, J.; Willis, C. L.; Simpson, T. J.; Crump, M. P. *J. Mol. Biol.* **2009**, *389*, 511.

1 (24) Sørensen, J. L.; Hansen, F. T.; Sondergaard, T. E.; Staerk, D.;
2 Lee, T. V.; Wimmer, R.; Klitgaard, L. G.; Purup, S.; Giese, H.;
3 Frandsen, R. J. N. *Environ. Microb.* **2012**, *14*, 1159.
4
5
6
7
8
9
10
11
12
13
14
15
16
17
18
19
20
21
22
23
24
25
26
27
28
29
30
31
32
33
34
35
36
37
38
39
40
41
42
43
44
45
46
47
48
49
50
51
52
53
54
55
56
57
58
59
60



Unable to Convert Image

The dimensions of this image (in pixels) are too large to be converted. For this image to convert, the total number of pixels (height x width) must be less than 40,000,000 (40 megapixels).

Figure 2

Unable to Convert Image

The dimensions of this image (in pixels) are too large to be converted. For this image to convert, the total number of pixels (height x width) must be less than 40,000,000 (40 megapixels).

Figure 3